Journal of Colloid and Interface Science **243,** 208–218 (2001)
doi:10.1006/jcis.2001.7840, available online at http://www.idealibrary.com on IDEAL®

Dynamic Cycling Contact Angle Measurements: Study of Advancing and Receding Contact Angles

C. N. C. Lam,* R. H. Y. Ko,† L. M. Y. Yu,† A. Ng,† D. Li,* M. L. Hair,* and A. W. Neumann*,[1]

*Department of Mechanical and Industrial Engineering, University of Toronto, 5 King's College Road, Toronto, Ontario, Canada M5S 3G8; and †Department of Chemical Engineering and Applied Chemistry, University of Toronto, 200 College St., Toronto, Ontario, Canada M5S 3E5

Received November 13, 2000; accepted July 14, 2001

Dynamic cycling contact angle (DCCA) measurements of six liquids from two homologous series (i.e., alkanes and alcohols) on FC-732-coated silicon wafer surfaces were performed using automated axisymmetric drop shape analysis-profile (ADSA-P). Unlike the previous one-cycle measurements that have been made in a number of studies, these cycling contact angle measurements provide more information on the mechanisms of contact angle hysteresis θ_{hyst}. Both the advancing contact angles θ_a (except for the one measured from the first cycle) and the receding contact angles θ_r obtained from different cycles were found to be time-dependent. By comparing the results between cycles, were obtained θ_a and θ_r values at some specific drop radii. It was found that both θ_a and θ_r decreased with increasing number of cycles. Furthermore, both θ_a and θ_r values obtained at the larger contact radius were larger than those obtained at the smaller radius. The result is plausible in terms of liquid sorption and/or retention by the solid surface: the solid surface modification by the liquid increases with longer solid/liquid contact, leading to smaller values of θ_a and θ_r. It was also found that contact angle hysteresis θ_{hyst}, the difference between θ_a and θ_r at each radius, increased initially and then leveled off with increasing number of cycles. The result suggests that processes which occurred on the polymer surface during the experiment, such as liquid sorption and evaporation, will eventually approach a steady state and hence lead to constant hysteresis of the contact angle. This supports the contention that liquid sorption and/or retention is a likely cause of the time dependence of contact angle hysteresis (as well as advancing and receding contact angles). All θ_a data obtained beyond the first cycle and all θ_r data reflect liquid sorption and/or retention by the solid and are therefore not a property of the solid alone. Therefore, only θ_a obtained in the first cycle (on the dry solid) should be used in the calculation of the surface energetics of solids.

Key Words: **dynamic cycling contact angle; advancing contact angle; receding contact angle; contact angle hysteresis; liquid sorption; liquid retention; surface tension; axisymmetric drop shape analysis.**

1. INTRODUCTION

Contact angle hysteresis θ_{hyst}, which is the difference between advancing contact angle θ_a and receding contact angle θ_r, has been studied extensively in the past few decades. In the past, researchers have attributed contact angle hysteresis to surface roughness (1–6) and heterogeneity (7–14). Later, some papers attributed contact angle hysteresis to metastable states (10, 13, 15–22). In more recent studies, Schwartz and Garoff (13, 14) found that contact angle hysteresis is strongly dependent on the patch structure of the surface, whereas McCarthy and his co-workers (18–20) related it to molecular mobility and packing as well as roughness of the surface in molecular dimensions.

In contrast with earlier studies, Sedev *et al*. (21, 22) attributed contact angle hysteresis to liquid penetration and surface swelling. In those studies, it was found that contact angle hysteresis depends on the chain length of the three alkanes tested and that hysteresis increased with decreasing chain length of the liquid. To further explore the effect of liquid penetration and surface swelling, we (23) performed systematic contact angle measurements on a well-prepared, dry, inert, and hydrophobic solid surface with two homologous series of liquids, the *n*-alkanes and the 1-alkyl alcohols. In that study, the receding contact angle was found to decrease with time, suggesting liquid sorption and surface swelling. An initial receding contact angle θ_{ri} (which is expected to reflect the receding angle before sorption starts) was extrapolated back to time of zero contact t_0 by least-squares regression in each experiment. It was found that contact angle hysteresis decreases with increasing chain length of the liquid molecules for both the alkane and the alcohol series. It vanished when the chain length was extrapolated to infinity. From these findings, the authors suggested that the penetration of liquid into the solid surface, or at least the retention of liquid, is presumably the cause of contact angle hysteresis on the type of solid surface studied. It was concluded that the common practice of using advancing contact angles in surface energetic calculations and disregarding the receding contact angles would be justified if contact angle hysteresis could be attributed totally to liquid sorption.

[1] To whom correspondence should be addressed. Fax: (416) 978-7753. E-mail: neumann@mie.utoronto.ca.

0021-9797/01 $35.00

It is the purpose of this study to further investigate the roles of liquid sorption and/or retention as causes of contact angle hysteresis. In many studies (24–26), advancing contact angles are taken to be equilibrium contact angles and have been used in conjunction with Young's equation as a means of characterizing solid surface energetics. The strategy of using low-rate advancing contact angles may alleviate the effect of equilibrium spreading pressure, local irregularities, and defects of the surface. Receding contact angles on a dry surface are experimentally as well as conceptually inaccessible. To the extent that receding contact angles reflect liquid retention by the solid, they are not a property of the solid alone (23) and cannot be used to characterize the dry solid surface. To further pin down the effect of liquid sorption and/or retention as a frequent cause of contact angle hysteresis, we extend the previous study by repeating the advancing and receding procedures with at least 12 cycles in each experiment on the same surface.

2. EXPERIMENTAL

2.1. Materials (Solid Surfaces and Liquids)

A fluorochemical coating, FC-732, was purchased from 3M Canada (London, Ontario; Product ID 98-0212-1124-2). This fluorocarbon coating was chosen because of its inertness and low surface tension ($\sim$12 mJ/m^2). FC-732 contains the same film-forming chemical as the FC-721 and FC-722 fluorocarbons used in other studies (21, 22, 27–31), but it uses a perfluorobutyl methyl ether rather than perfluorooctane (FC-721) and 1,1,2,-trichloro-1,2,2,-trifluoroethane (FC-722). Therefore, some of the results from this study can be compared with those from FC-721 and FC-722. The FC-732-coated surfaces were prepared by a dip-coating technique (24) on cleaned and dried silicon wafers. Silicon wafers ⟨100⟩ (Silicon Sense, Naschua, N.H.; thickness 525 ± 50 μm) were selected as the substrate for the contact angle measurements since they are smooth and rigid. They were cut into rectangular shapes of about 2.5×5 cm from the original circular discs, which were about 10 cm in diameter. For low-rate dynamic contact angle measurements using axisymmetric drop shape analysis-profile (ADSA-P), the liquid was supplied to the sessile drop from below the wafer surfaces using a motorized syringe device (28, 32). To facilitate the experimental procedure, a hole of 1-mm diameter was drilled in the center of each wafer by using an SMS $-$ 0.027 diamond drill bit from Lunzer (New York). The wafer surfaces were then rinsed with acetone to remove dirt and fingerprints. After drying, they were soaked in chromic acid for at least 24 h, rinsed with doubly distilled water, and dried under a heat lamp before the coating process. To avoid leakage between a stainless steel needle (Chromatographic Specialties, Brockville, Ontorio; N723 needles pt. # 3, H91023) and the hole on the wafer surface, Teflon tape was wrapped around the end of the needle before it was inserted into the hole. Since the duration of each experiment was over two hours, the liquid drop and the solid surface were enclosed in a sealed optical glass container.

The solid surfaces were prepared by a dip-coating technique: the clean surface was immersed vertically into the 2% FC-732 solution at a speed of 4×10^{-2} cm/s and the surface was soaked for 20 min in the solution. The surface was then withdrawn at the same speed as that used for immersion and was dried at room temperature. This technique produces high-quality-coated surfaces; the surface roughness is on the order of nanometers or less.

The liquids used in this study are the three alkanes *n*-nonane, *n*-dodecane, and *n*-hexadecane and the corresponding alcohols, 1-hexanol, 1-nonanol, and 1-undecanol. Suppliers, purity, and the relevant properties of these liquids are given in Table 1. All measurements were performed at $23.0^\circ\text{C} \pm 0.5^\circ\text{C}$.

2.2. Methods and Procedures

Axisymmetric Drop Shape Analysis-Profile (ADSA-P) is a technique for determining liquid–fluid interfacial tensions and contact angles from the shape of axisymmetric menisci, i.e.,

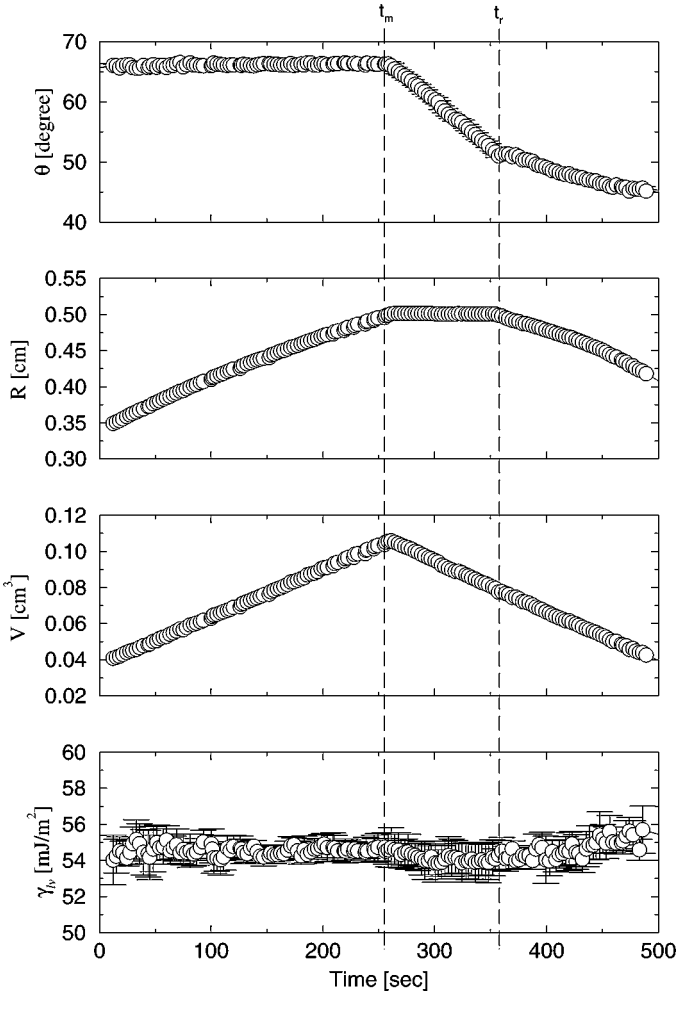

FIG. 1. Low-rate dynamic 1-cycle contact angle measurement of formamide on poly(methyl methacrylate/*n*-butyl methacrylate)-coated silicon wafer.

TABLE 1
Supplier, Purity, and Properties of Liquids Used

Liquid	Supplier	% Purity	Density (g/cm^3)	γ_{lv} (mJ/m^2)[a]
Alkanes				
n-Nonane	Aldrich	99+	0.718	22.62
n-Dodecane	Aldrich	99+	0.750	25.13
n-Hexadecane	Aldrich	99+	0.773	27.62
Alcohols				
1-Hexanol	Aldrich	98	0.814	26.05
1-Nonanol	Aldrich	98	0.827	27.55
1-Undecanol	Sigma-Alrich	99	0.830	28.88

[a] Measured by axisymmetric drop shape analysis: pendant drop at 23.0°C ± 0.5°C.

from sessile as well as pendant drops. The underlying ADSA strategy and details of the methodology and experimental set-up can be found elsewhere (27, 33–35).

The advancing and receding contact angles reported in this paper were determined by sessile drop experiments, which were analyzed by ADSA-P. During the experiment, the temperature and relatively humidity were 23.0°C ± 0.5°C and approximately 45%, respectively.

In this study, the contact angle measurements were conducted dynamically just as in a number of previous studies that focused only on advancing contact angles (27, 28, 36, 37). Advantages of measuring dynamic contact angles instead of static contact angles were discussed in a previous study (23).

In the sessile drop experiments, a bubble level was first used to level the surface stage. A test surface was then carefully placed on the surface stage so that the needle would pass through the hole in the sample surface. The needle was adjusted so that its tip was just above the test surface. To ensure that the drop increased axisymmetrically in the center of the image field and did not hinge on the lip of the hole when liquid was supplied from below the surface, an initial liquid drop of about 0.4 cm radius was carefully deposited from *above* to cover the hole on the surface. To seal the drop-surface system, an optical quartz cuvette was placed on the platform to cover the system. A few drops of the liquid used was then deposited at the edge of the glass

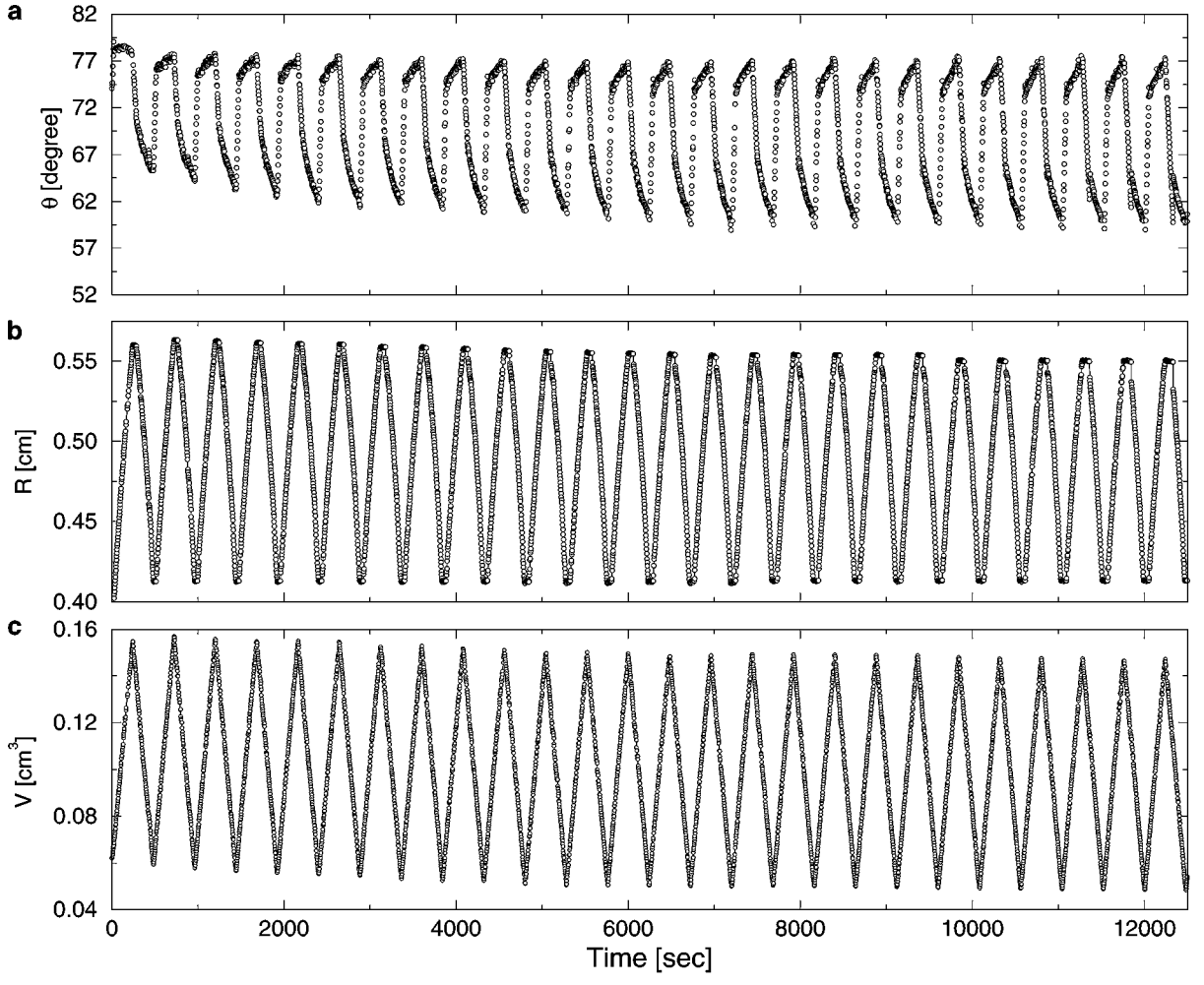

FIG. 2. Dynamic cycling contact angles with *n*-hexadecane on FC-732-coated surface.

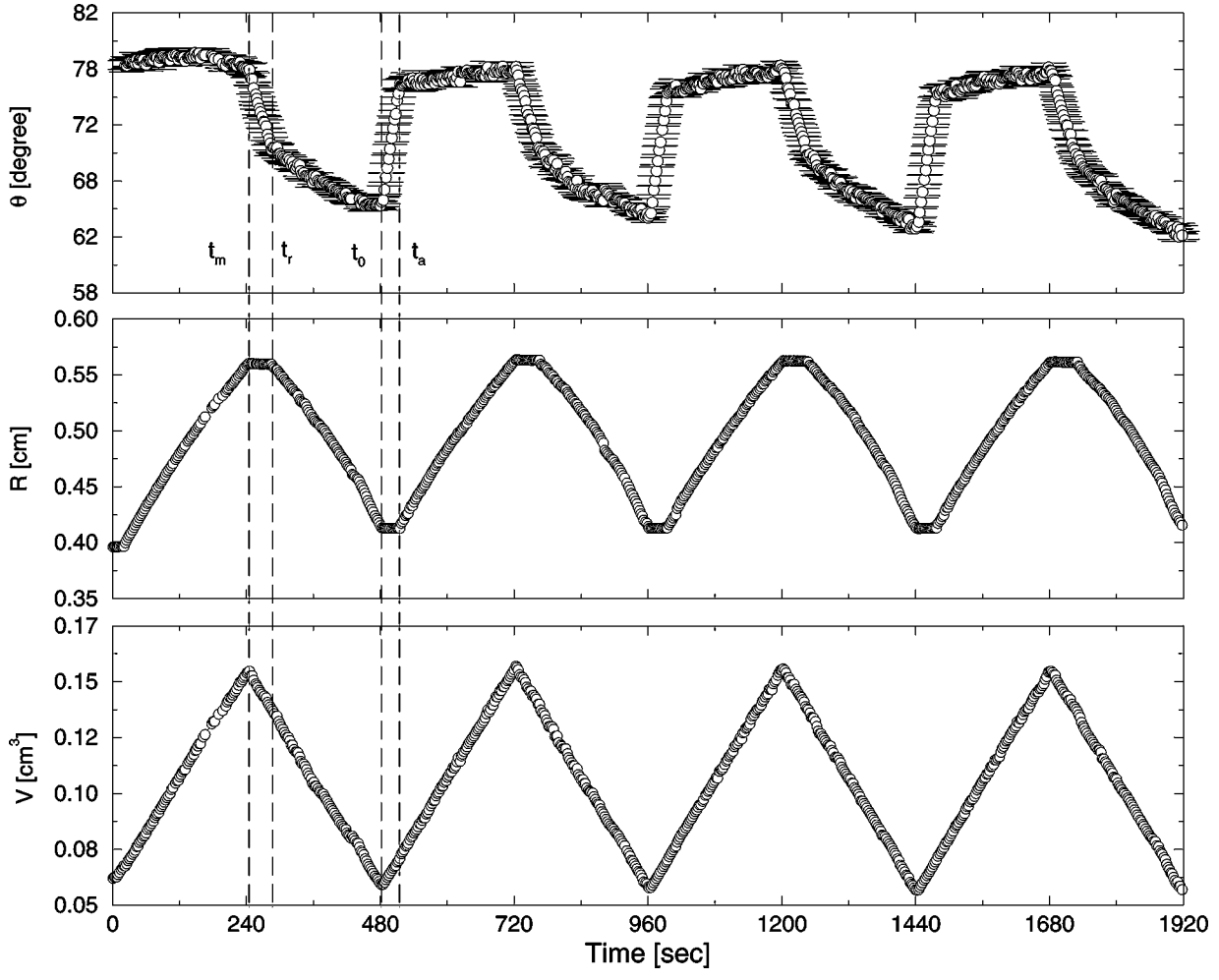

FIG. 3. The first four cycles from a dynamic cycling contact angle experiment with *n*-hexadecane on FC-732-coated surface.

container to seal the gap between the platform and the cuvette. This enclosure minimized evaporation of the liquid and created a saturated vapor environment for the drop–surface system. The motor-driven syringe (2.5 ml, #1002, Gastight, Hamilton Co., USA) was connected to a stepper motor (Model 18705, Oriel Corp., USA) by an aluminum coupling. The motor was then set to a specific speed to control the volumetric flow rate of the liquid to or from the sessile drop. The mechanism pushed the syringe plunger during the advancing procedure and pulled it during the receding procedure, leading to an increase and decrease of drop size, respectively. Images of the growing and shrinking drop were then recorded by the computer, typically at a rate of a picture every 2 s. In this study, the advancing and receding processes were repeated at least 12 times, taking the system through 12 cycles.

3. RESULTS AND DISCUSSION

Low-rate dynamic contact angles of different liquids on various well-prepared polymeric films and coatings have been extensively studied in our laboratory in the past few years. However, except for one recent study (23), the focus was on the advancing contact angle. Receding contact angles were essentially disregarded. In Fig. 1, a typical result of both advancing and receding contact angle measurements from a dynamic one-cycle contact angle experiment of formamide on poly(methyl methacrylate/*n*-butyl methacrylate)-coated silicon wafer is illustrated. Contact angle θ, surface tension γ_{lv}, drop volume V, and drop radius R (see Fig. 1) are plotted as a function of time. For convenience, these results are divided into three domains (23). The first domain ranges from the beginning of the experiment to time t_m when the motor was switched to reverse and the liquid started to flow back to the syringe. It can be seen from this domain that as the drop radius and volume increase, the advancing contact angles θ_a are essentially constant. The second domain ranges from time t_m to time t_r, i.e., the point in time when the contact line of the drop starts to recede. This domain is characterized by a constant radius and a rapid decrease in contact angle. The domain represents the transition from advancing to receding contact angles, i.e., the period during which the three-phase line

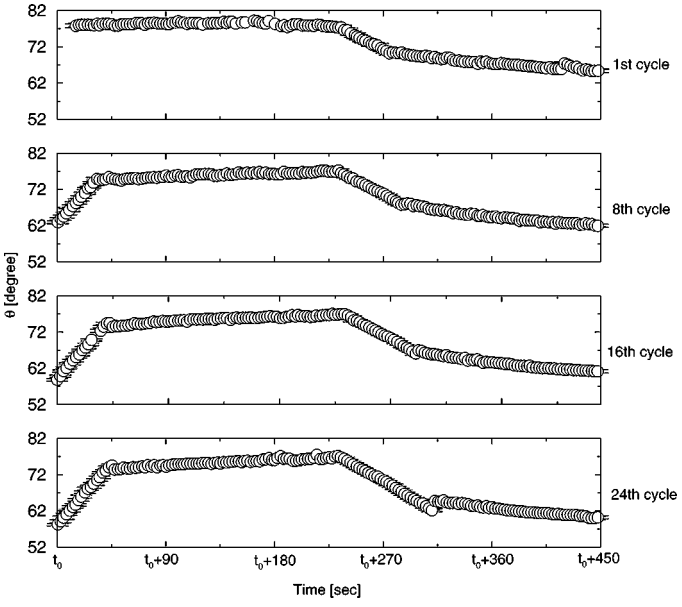

FIG. 4. The first, 8th, 16th, and 24th cycles from a dynamic cycling contact angle experiment with *n*-hexadecane on FC-732-coated surface.

is stationary. The third domain ranges from time t_r to the end of the experiment. This domain is characterized by decreasing radius and a decrease of the receding contact angle θ_r. This pattern strongly suggests liquid retention by the solid, as the receding angle decreases with increasing solid–liquid contact time. This contact angle pattern is typical of a large number of solid–liquid systems. We have argued in the past (38) that there is a correlation between line tension and contact angle hysteresis on rough as well as heterogeneous surfaces. For smooth and homogeneous surfaces such as we studied here, those model considerations do not provide an explanation for the existence of contact angle hysteresis. Thus, the identification of sorption/retention as a common cause for contact angle hysteresis is entirely compatible with the idea of a correlation between line tension and contact angle hysteresis. The implication is that, if there were no sorption/retention of liquid, there would be no contact angle hysteresis, as we also argued recently (23).

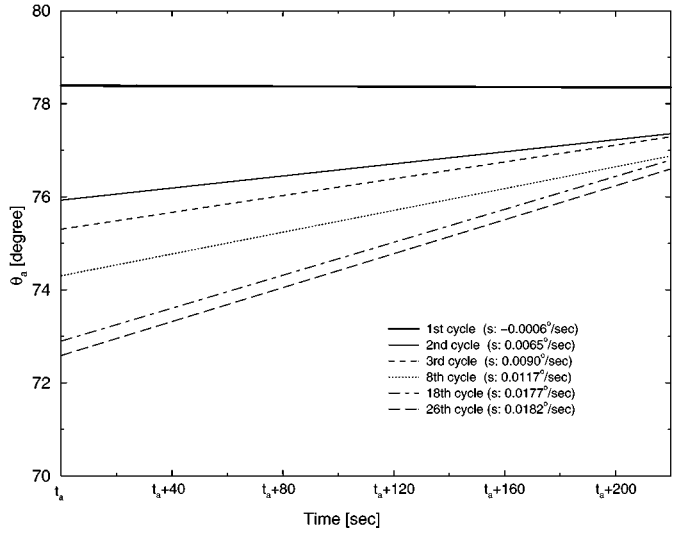

FIG. 5. Comparison of the slopes of the advancing contact angle obtained from different cycles (*n*-hexadecane on FC-732-coated surface).

3.1. *Alkanes*

Figure 2 illustrates a typical result obtained from a cycling experiment for *n*-hexadecane on an FC-732-coated surface. In this experiment, 26 cycles of advancing and receding contact angle measurements were performed consecutively in approximately $3\frac{1}{2}$ h. A complete cycle consists of expansion of the liquid drop from the initial volume/radius to the final (maximum) volume/radius and contraction back to the initial point, which can be identified from both the radius and the volume plots as shown in Figs. 2b and 2c. At the end of the first cycle, wetted circular domains of the solid surface nearest the point where liquid retraction starts will have had the shortest contact time with the liquid, while the domains closer to the center of the drop will

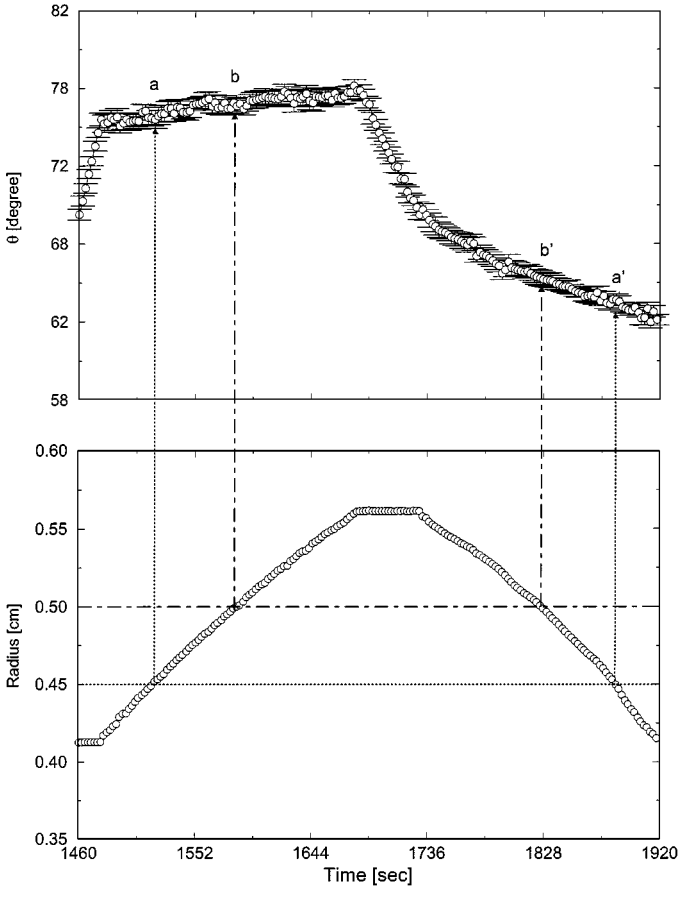

FIG. 6. A typical cycle (the fourth cycle in this case) in a cycling experiment. a and a′ denote the advancing and receding contact angles obtained from $R = 0.45$ cm, respectively. b and b′ denote the advancing and receding contact angles obtained from $R = 0.50$ cm, respectively.

have had longer contact times. In the contact angle plot (Fig. 2a), the maximum value in each cycle represents the advancing contact angle obtained when the liquid/solid contact time was the shortest and the minimum value represents the receding contact angle obtained when the liquid/solid contact time was the longest. It can be seen in this plot that the maximum values of the first 10 cycles decrease with the increase of the number of cycles and remain essentially constant beyond the 10th cycle. The minimum values decrease with the increasing number of cycles and the extent of the decrease becomes smaller as the number of cycles increases. It is apparent that both advancing and receding contact angles decrease with increasing contact time between solid and liquid.

Figure 3 shows the first four cycles of the same cycling experiment in more detail. For the repeated cycling experiments, an additional domain that ranges from time t_0 to time t_a is introduced. This domain is characterized by constant radius and a rapid increase in the contact angle with increasing drop volume. It represents the transition from receding to advancing contact angles. Time t_0 is where the motor was switched back to the forward mode and the liquid started to flow back into the sessile drop, starting the next cycle. Time t_a designates the point where the three-phase line starts to advance again. As shown in Fig. 3, the advancing contact angle in the second cycle is time-dependent: it increases as the drop radius increases. Increases in the third and the fourth cycles become more pronounced. It appears from Fig. 2 that the slope of the advancing contact angles increases progressively from cycle to cycle. Similarly, the slope of the receding contact angles increases gradually with increasing number of cycles.

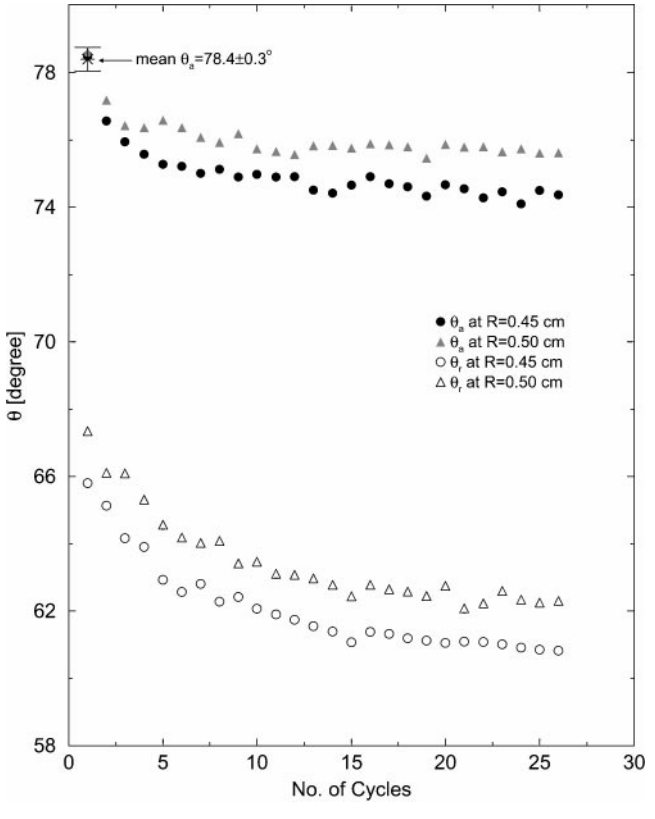

FIG. 7. The advancing and receding contact angles of *n*-hexadecane on a FC-732-coated surface obtained for the two specific radii ($R = 0.45$ and 0.50 cm) versus the number of cycles; mean θ_a denotes the averaged value of advancing contact angles measured from the first cycle.

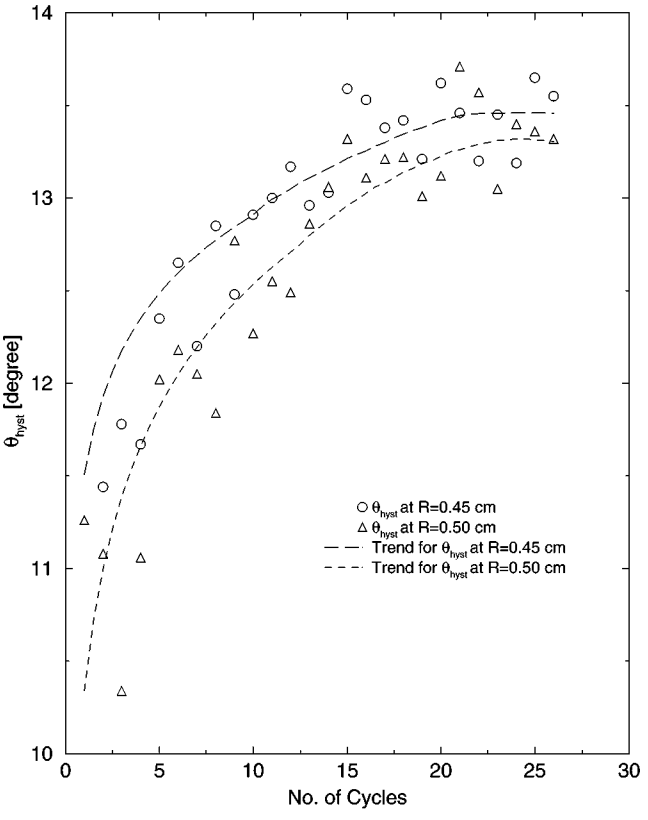

FIG. 8. Contact angle hysteresis θ_{hyst} of *n*-hexadecane on FC-732-coated surface, together with the trends obtained at the two specific radii ($R = 0.45$ and 0.50 cm) versus the number of cycles.

For comparison, the 1st, 8th, 16th, and 24th cycles are displayed in Fig. 4. It can be seen that the slope for the advancing contact angle increases with increasing number of cycles. The time-dependent advancing contact angles obtained beyond the first cycle indicate that the solid surface has changed, presumably due to liquid sorption and/or liquid retention during the previous cycle/cycles. Figure 5 compares the slopes obtained from linear regression of different cycles. The slope for the first cycle is expected to be zero but actually is finite but very small ($\sim -0.0006^\circ$/s), probably reflecting minor inhomogeneity of the solid surface. It can be seen that the values of advancing contact angles decrease with the increase of the number of cycles (i.e., the line for advancing contact angles shifts down to lower values). The decrease is pronounced in earlier cycles, especially between the first and the second cycles. The result reveals that the hydrophobicity of the surface (or the contact angle) decreases from cycle to cycle; i.e., the solid surface is modified due to the

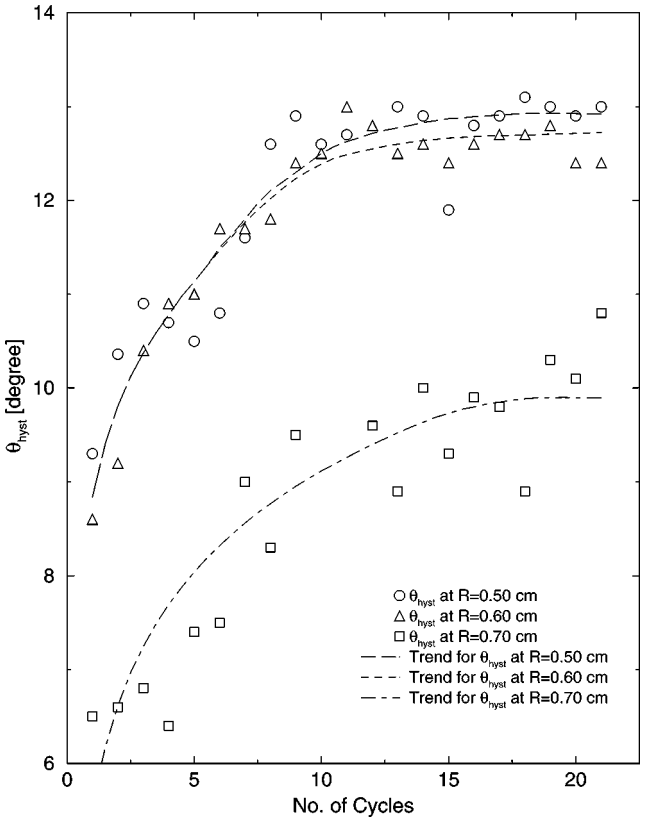

FIG. 9. Contact angle hysteresis θ_{hyst} of *n*-dodecane on FC-732-coated surface, together with the trends obtained at the three specific radii ($R = 0.50$, 0.60, and 0.70 cm) versus the number of cycles.

contact with the liquid. Liquid sorption and/or retention is the most likely cause for this modification. When the liquid and the solid are brought into contact, liquid molecules may penetrate into and/or be retained on the solid, and hence will change the properties of the surface. A more or less irreversible change of the solid surface purely due to a surface interaction seems less likely because it will normally be polymer chain segments and not whole polymer chains that constitute the surface. However, it cannot be excluded that liquid penetration into the solid may possibly lead to a reorientation of molecular chains or a change in the packing of polymer chains in the polymeric film. Since the contact angle is a measure of surface characteristics, the decrease of advancing contact angles reflects an increase of surface tension. It can also be observed that after the first cycle the slope increases with increasing number of cycles. After the 18th cycle, the slopes become essentially constant, but the contact angles still decrease overall. This pattern might suggest that there is actually more than one operative mechanism. For instance, the pattern might be caused by a competition between liquid sorption of the polymer surface when in contact with the liquid and evaporation from the polymer surface when not in contact with the liquid. These processes can have different rate constants, and the actual rates of sorption and evaporation will depend on the state of saturation of the solid by the liquid. Elucidation of such matters is beyond the scope of this study.

As noted previously (23), it is conceptually impossible to measure a receding contact angle on a dry solid surface. Thus the receding contact angle obtained in the first cycle is time-dependent, as shown in Fig. 4. Although there is no obvious change in the slope for the receding contact angle, the overall receding contact angle decreases with increasing number of cycles. It can also be seen in Fig. 4 that the periods of the stationary three-phase line increase. The three-phase line starts to advance/recede at a lower advancing/receding contact angle in the later cycles. This is a consequence of the design of the experiment, which uses a constant liquid volume flow rate. Furthermore, it can be observed in the 16th and the 24th cycles (Fig. 4) that "slip–stick" occurs at the end of the advancing–receding transition, i.e., at the beginning of the receding domain. The three-phase contact line sticks at the end of the advancing-receding transition where the contact angle keeps decreasing; the three-phase line slips suddenly and the contact angle jumps to a higher value. The jump becomes more pronounced as the number of cycles increases. Apparently, liquid molecules manage to anchor themselves sufficiently firmly on the solid where the three-phase line is stationary so that the bulk liquid can resist the flow until a sufficiently large mechanical stress builds up.

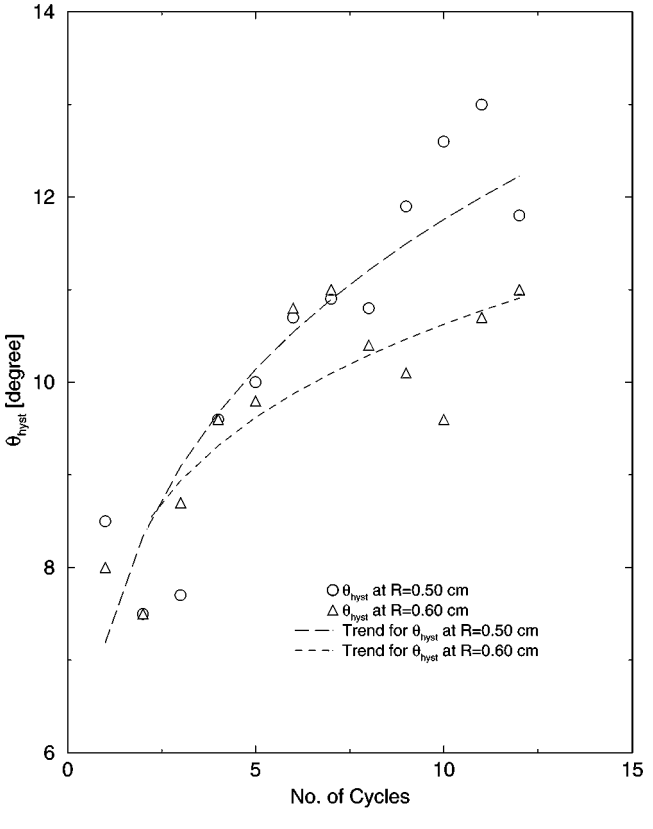

FIG. 10. Contact angle hysteresis θ_{hyst} of *n*-nonane on FC-732-coated surface, together with the trends obtained at the two specific radii ($R = 0.50$ and 0.60 cm) versus the number of cycles.

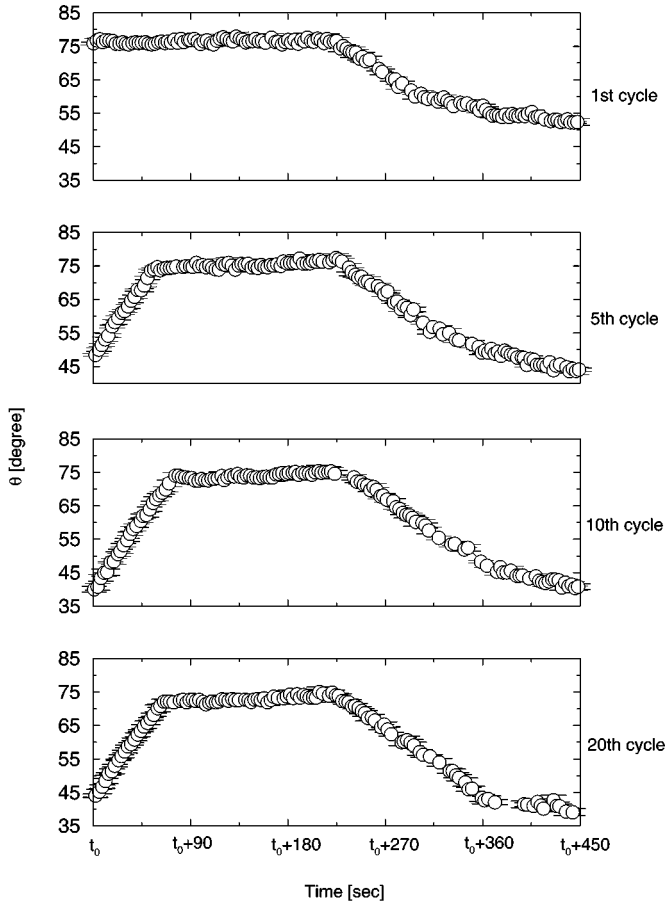

FIG. 11. The first, 5th, 10th, and 20th cycles from a dynamic cycling contact angle experiment with 1-nonanol on FC-732-coated surface.

In view of the fact that both the advancing contact angle θ_a and the receding contact angle θ_r are time-dependent (except for the advancing contact angle in the first cycle), the corresponding advancing and receding contact angles at *specific radii* have been chosen to compare the contact angles from cycle to cycle (Fig. 6). For *n*-hexadecane, radii at $R = 0.45$ and 0.50 cm are chosen and the corresponding advancing and receding contact angles are determined. Figure 6 illustrates a typical cycle (the fourth cycle in this case). The advancing and receding contact angles at $R = 0.45$ cm are denoted by a and a', respectively. Similarly, b and b' indicate the corresponding advancing and receding angles at $R = 0.50$ cm. Again, it should be noted that the solid/liquid contact time increases with decreasing drop radius.

Figure 7 shows the advancing and receding angles obtained from the two specific radii as a function of the number of cycles. The mean θ_a value for the first cycle, together with its 95% confidence limit, is also given in this figure. It can be seen clearly that both θ_a and θ_r data obtained at the two radii are decreasing with increasing number of cycles. As the number of cycles increases, both the solid–liquid contact time and the hydrophilicity of the solid surface increase. It is plausible that liquid sorption and/or retention causes a decrease of both θ_a and θ_r. Furthermore, it can be seen from Fig. 7 that values of θ_a and θ_r obtained at the outer radius ($R = 0.50$ cm in this case) are higher than those obtained at the inner radius ($R = 0.45$ cm). This is expected since the time of solid/liquid contact is longer at the inner radius than at the outer radius, and thus, the solid surface would be more hydrophilic at the inner radius. The results strongly suggest that the time dependence of contact angles on these relatively smooth and homogeneous surfaces is most likely caused by liquid retention/sorption.

The contact angle hysteresis θ_{hyst}, which is the difference between θ_a and θ_r obtained at each radius for each cycle, is plotted against the number of cycles in Fig. 8. A trend line for θ_{hyst} at each radius is also displayed in this figure. It can be seen that the contact angle hysteresis increases rapidly for the first 15 cycles and becomes essentially constant beyond the 15th cycle. In addition, it can be observed that the trend line obtained at the inner radius is above the one obtained at the outer radius; in other words, the θ_{hyst} at the inner radius is larger than that obtained at the outer radius. This is expected because surface modification should be greater for longer solid–liquid contact times.

Dynamic cycling contact angle measurements with *n*-dodecane and *n*-nonane produced results that are quite similar to those for *n*-hexadecane. For *n*-dodecane, θ_a and θ_r were determined from three radii: $R = 0.50$, 0.60, and 0.70 cm. The

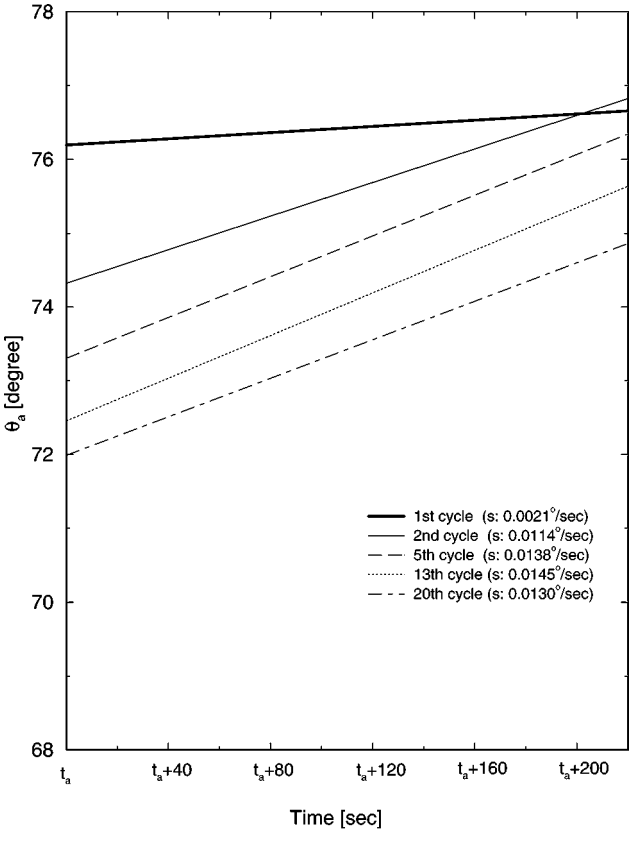

FIG. 12. Comparison of the slopes of the advancing contact angle obtained from different cycles (1-nonanol on FC-732-coated surface).

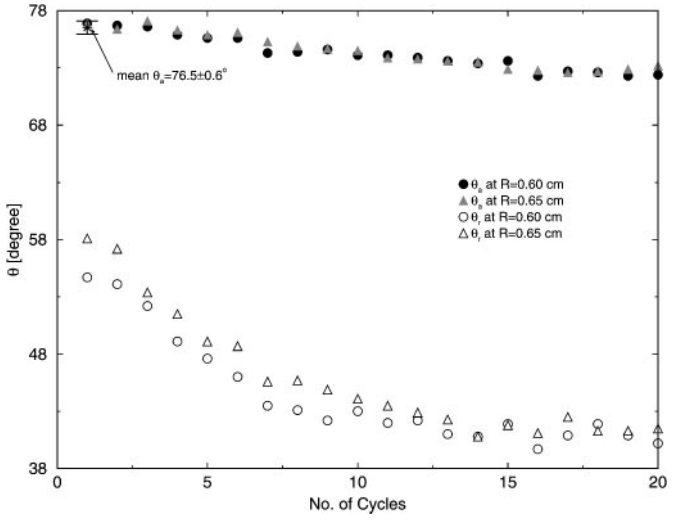

FIG. 13. The advancing and receding contact angles of 1-nonanol on a FC-732-coated surface obtained for the two specific radii ($R = 0.60$ and 0.65 cm) versus the number of cycles; mean θ_a denotes the average value of advancing contact angles measured from the first cycle.

pattern of the plot for θ_a and θ_r versus the number of cycles (not shown here) is similar to the one in Fig. 7. Both θ_a and θ_r obtained from the outer radius have higher values than those obtained from the inner radius. Figure 9 shows the plot of the contact angle hysteresis obtained at the three radii as a function of the number of cycles. It can be seen clearly from this plot that θ_{hyst} value determined at $R = 0.50$ and 0.60 cm increase initially and level off beyond the 10th cycle, as illustrated by the trend lines. The result implies that contact angle hysteresis will eventually approach a steady state. The results suggest that, after a certain number of cycles of advancing and receding, the rates of liquid retention–evaporation or sorption would balance each other. It appears indeed that liquid sorption and/or retention by the solid are responsible for the time dependence of contact angle hysteresis phenomena. The results for *n*-nonane, shown in Fig. 10, confirm this conclusion further. However, due to experimental limitations (fast evaporation), only 12 cycles could be obtained. Apparently, this was not sufficient to detect the leveling-off of the trend lines.

Because of the experimental limitations, it would be misleading to make any comparison among Figs. 8–10. The rate of movement of the three-phase line cannot be controlled in our current setup, so the times of the solid–liquid contact at the same radius size for the three alkanes are also different. Since hysteresis is strongly dependent on solid–liquid contact time, it is not appropriate to compare θ_{hyst} or the trend line from one liquid to the next, even if they are obtained at the same radius. Furthermore, previous studies (21–23) concluded that contact angle hysteresis depends on the molecular size of the liquids. Seemingly, Figs. 8–10 do not bear this out. Again, the comparison must be rejected. The duration of a cycle at constant volume flow rate depends on the contact angle, which changes from liquid to liquid and also with contact time for one and the same liquid.

3.2. Alcohols

Figure 11 illustrates the first, 5th, 10th, and 20th cycles chosen from a cycling contact angle measurement with 1-nonanol. Similar phenomena are observed: the advancing contact angles in the first cycle are essentially constant; θ_a beyond the first cycle is time-dependent; the advancing–receding transition period increases with the increase of the number of cycles; and the advancing and receding periods generally decrease with increasing number of cycles, because the contact angles decrease due to liquid contact. The slopes of advancing contact angle (obtained by linear regression) for various cycles with 1-nonanol are displayed in Fig. 12. As with the alkanes, the greatest change in slope occurs from the first to the second cycle, which implies that the surface modification is the most pronounced upon first contact with the liquid. Although there is no significant change in the slope from the 5th, 13th, and 20th cycles (see Fig. 12), the advancing contact angles decrease with the number of cycles. For 1-nonanol, θ_a and θ_r at $R = 0.60$ and 0.65 cm are plotted against the number of cycles in Fig. 13. The mean θ_a obtained by averaging the advancing contact angles measured in the first advancing procedure, together with its 95% confidence limit, is also given in Fig. 13. It should be noted that the scales in Figs. 7 and 13 are different, and therefore, the difference

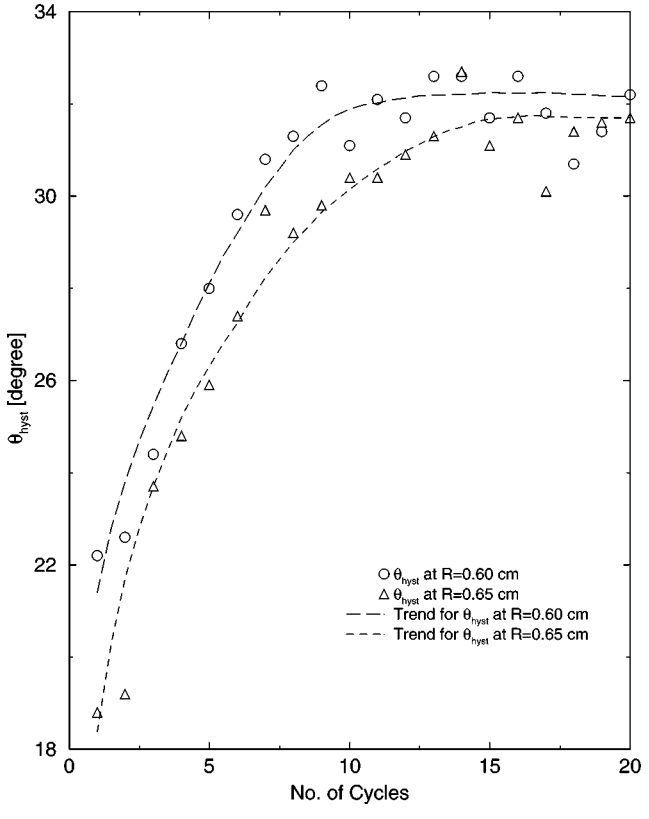

FIG. 14. Contact angle hysteresis θ_{hyst} of 1-nonanol on FC-732-coated surface, together with the trends obtained at the two specific radii ($R = 0.60$ and 0.65 cm), versus the number of cycles.

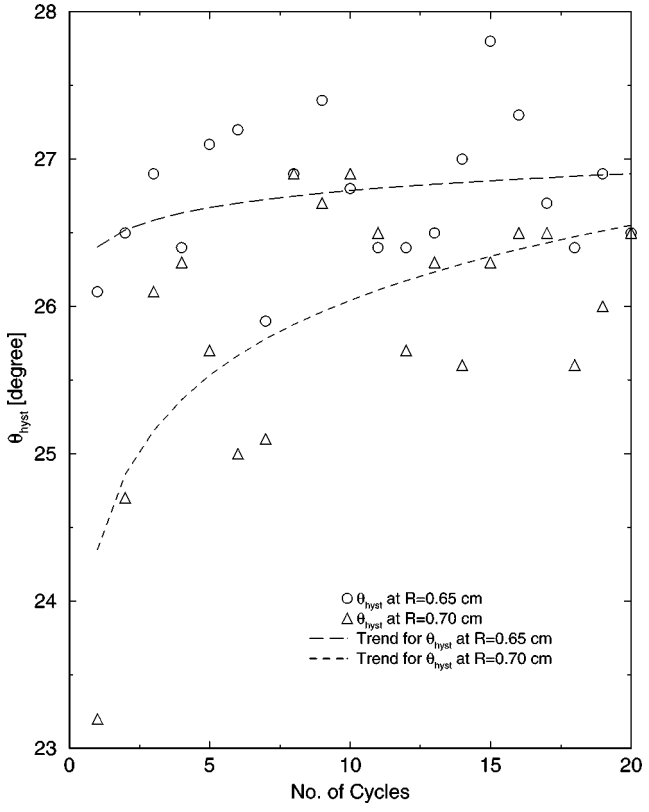

FIG. 15. Contact angle hysteresis θ_{hyst} of 1-undecanol on FC-732-coated surface, together with the trends obtained at the two specific radii ($R = 0.65$ and 0.70 cm), versus the number of cycles.

between θ_a values obtained from $R = 0.60$ and 0.65 cm is not noticeable. However, it can be seen from Fig. 13 that θ_r values obtained at $R = 0.60$ are smaller than those obtained at $R = 0.65$ cm. Figure 14 shows the contact angle hysteresis plot for 1-nonanol. The trend lines indicate that θ_{hyst} approaches a steady state somewhat faster for the smaller radius of contact, in agreement with the expectation that this state should be reached earlier, the longer the time of liquid contact in each cycle.

The contact angle hysteresis plot for 1-undecanol is given in Fig. 15. The data show more scatter, but the general pattern remains. For 1-hexanol, θ_a and θ_r well read off at three radii: $R =$ 0.50, 0.55, and 0.60 cm. No specific trend could be observed in the plot of contact angle hysteresis vs. number of cycles, so the data is not shown. The contact angle hysteresis data obtained from each radius scatter within two degrees, instead of the trends that have been seen in other systems (c.f. Figs. 8–10, 14, and 15). This result is reasonable: 1-hexanol is a smaller molecule than the other two alcohols used in this study. Thus, the propensity of liquid sorption to take place in the solid–liquid system would be higher. Because of the relatively high vapor pressure of the 1-hexanol, it stands to reason that the two processes, sorption and evaporation, would balance each other quickly, leading to the observed steady state!

4. CONCLUSION

(1) On a well-prepared, inert, and hydrophobic surface, advancing contact angles (except for the one obtained from the first cycle) and receding contact angles reflect liquid sorption and/or retention. This conclusion is a consequence of the fact that contact angle hysteresis depends on solid–liquid contact time, presumably molecular size, and other properties of the liquid.

(2) The advancing and receding contact angles obtained from the outer radii (shorter solid–liquid contact time) are found to be greater than those obtained from the inner radii. This result is explained by liquid sorption and retention: the surface energy of the solid would increase when solid and liquid are brought into contact. Therefore, the hydrophilicity of the solid surface would increase with the increase of solid–liquid contact time.

(3) Contact angle hysteresis becomes constant after a certain period of advancing and receding, presumably due to the balancing of the rate of retention and of evaporation. The results confirm that, on the solid studied here, liquid sorption, penetration, and/or retention are likely causes of the time dependence of contact angle hysteresis.

(4) The results have shown that not only the receding contact angles but also the advancing contact angles obtained on a wetted surface (i.e., θ_a obtained after the first cycle) reflect an effect of the liquid. Therefore, only the advancing contact angle obtained on a dry surface (i.e., θ_a obtained from the first cycle) is appropriate in the calculation of surface energetics.

ACKNOWLEDGMENTS

This work was supported by the Natural Science and Engineering Research Council (NSERC) of Canada under Grant A8278. Financial support through a NSERC Postgraduate Scholarships (C.N.C.L) is gratefully acknowledged.

REFERENCES

1. Bartell, F. E., and Shepard, J. W., *J. Phys. Chem.* **57,** 211 (1953).
2. Johnson, Jr., R. E., and Dettre, R. H., *Adv. Chem. Ser.* **43,** 112 (1964).
3. Eick, J. D., Good, R. J., and Neumann, A. W., *J. Colloid Interface Sci.* **53,** 235 (1975).
4. Oliver, J. F., Huh, C., and Mason, S. G., *J. Adhes.* **8,** 223 (1977).
5. Oliver, J. F., Huh, C., and Mason, S. G., *Colloids Surf.* **1,** 79 (1980).
6. Oliver, J. F., and Mason, S. G., *J. Mater. Sci.* **15,** 431 (1980).
7. Good, F. J., *J. Am. Chem. Soc.* **74,** 5041 (1952).
8. Johnson, Jr., R. E., and Dettre, R. H., *J. Phys. Chem.* **68,** 1744 (1964).
9. Dettre, R. H., and Johnson, Jr., R. E., *J. Phys. Chem.* **69,** 1507 (1965).
10. Neumann, A. W., and Good, R. J., *J. Colloid Interface Sci.* **38,** 341 (1972).
11. Schwartz, L. W., and Garoff, S., *Langmuir* **1,** 219 (1985).
12. Marmur, A., *J. Colloid Interface Sci.* **168,** 40 (1994).
13. Decker, E. L., and Garoff, S., *Langmuir* **12,** 2100 (1996).
14. Decker, E. L., and Garoff, S., *Langmuir* **13,** 6321 (1997).
15. Derjaguin, B. V., *C. R. Acad. Sci., USSR* **51,** 361 (1946).
16. Johnson, Jr., R. E., and Dettre, R. H., *in* "Surface and Colloid Science" (E. Matijevic, Ed.), p. 85. Wiley–Interscience, New York, 1969.
17. Brandon, S., and Marmur, A., *J. Colloid Interface Sci.* **183,** 351 (1996).
18. Chen, W., and McCarthy, T. J., *Macromolecules* **30,** 78 (1997).

19. Fadeev, A. Y., and McCarthy, T. J., *Langmuir* **15,** 3759 (1999).
20. Youngblood, J. P., and McCarthy, T. J., *Macromolecules* **32,** 6800 (1999).
21. Sedev, R. V., Petrov, J. G., and Neumann, A. W., *J. Colloid Interface Sci.* **180,** 36 (1996).
22. Sedev, R. V., Budziak, C. J., Petrov, J. G., and Neumann, A. W., *J. Colloid Interface Sci.* **159,** 392 (1993).
23. Lam, C. N. C., Kim, N., Hui, D., Kwok, D. Y., Hair, M. L., and Neumann, A. W., *Colloids Surf. A Physicochem. Eng. Aspects* **189,** 265 (2001).
24. Li, D., and Neumann, A. W., *J. Colloid Interface Sci*. **148,** 190 (1992).
25. Li, D., and Neumann, A. W., *Adv. Colloid Interface Sci.* **39,** 299 (1992).
26. Kwok, D. Y., and Neumann, A. W., *Adv. Colloid Interface Sci.* **81,** 167 (1999).
27. Kwok, D. K., Gietzelt, T., Grundke, K., Jacobasch, H.-J., and Neumann, A. W., *Langmuir* **13,** 2880 (1997).
28. Kwok, D. Y., Lin, R., Mui, M., and Neumann, A. W., *Colloids Surf. A Physicochem. Eng. Aspects* **116,** 63 (1996).
29. Del Rio, O. I., Kwok, D. Y., Wu, R., Alvarez, J. M., and Neumann, A. W., *Colloids Surf. A Physicochem. Eng. Aspects* **143,** 197 (1996).
30. Li, D., and Neumann, A. W., *J. Colloid Interface Sci.* **148,** 190 (1992).
31. Duncan, D., Li, D., Gaydos, J., and Neumann A. W., *J. Colloid Interface Sci.* **169,** 256 (1995).
32. Brandrup, J., "*Polymer Handbook*," 2nd ed. Wiley–Interscience, New York, 1975.
33. Rotenberg, Y., Boruvka, L., and Neumann, A. W., *J. Colloid Interface Sci.* **93,** 169 (1983).
34. Cheng, P., Li, D., Boruvka, L., Rotenberg, Y., and Neumann, A. W., *Colloids Surf.* **93,** 169 (1983).
35. Lahooti, S., del Rio, O. I., Cheng, P., and Neumann, A. W., *in* "Applied Surface Thermodynamics" (A. W. Neumann and J. K. Spelt, Eds.), p. 441. Dekker, New York, 1996.
36. Kwok, D. Y., Lam, C. N. C., Li, A., Leung, A., Wu, R., Mok, E., and Neumann, A. W., *Colloids Surf. A Physicochem. Eng. Aspects* **142,** 219 (1998).
37. Kwok, D. Y., Lam, C. N. C., Li, A., Zhu, K., Wu, R., and Neumann, A. W., *Polymer Eng. Sci.* **38,** 1675 (1998).
38. Gaydos, J., and Neumann, A. W., *in* "Applied Surface Thermodynamics" (A. W. Neumann and J. K. Spelt, Eds.), pp. 169–238. Dekker, New York, 1996.